Supplemental material

Lee et al., https://doi.org/10.1083/jcb.201811147

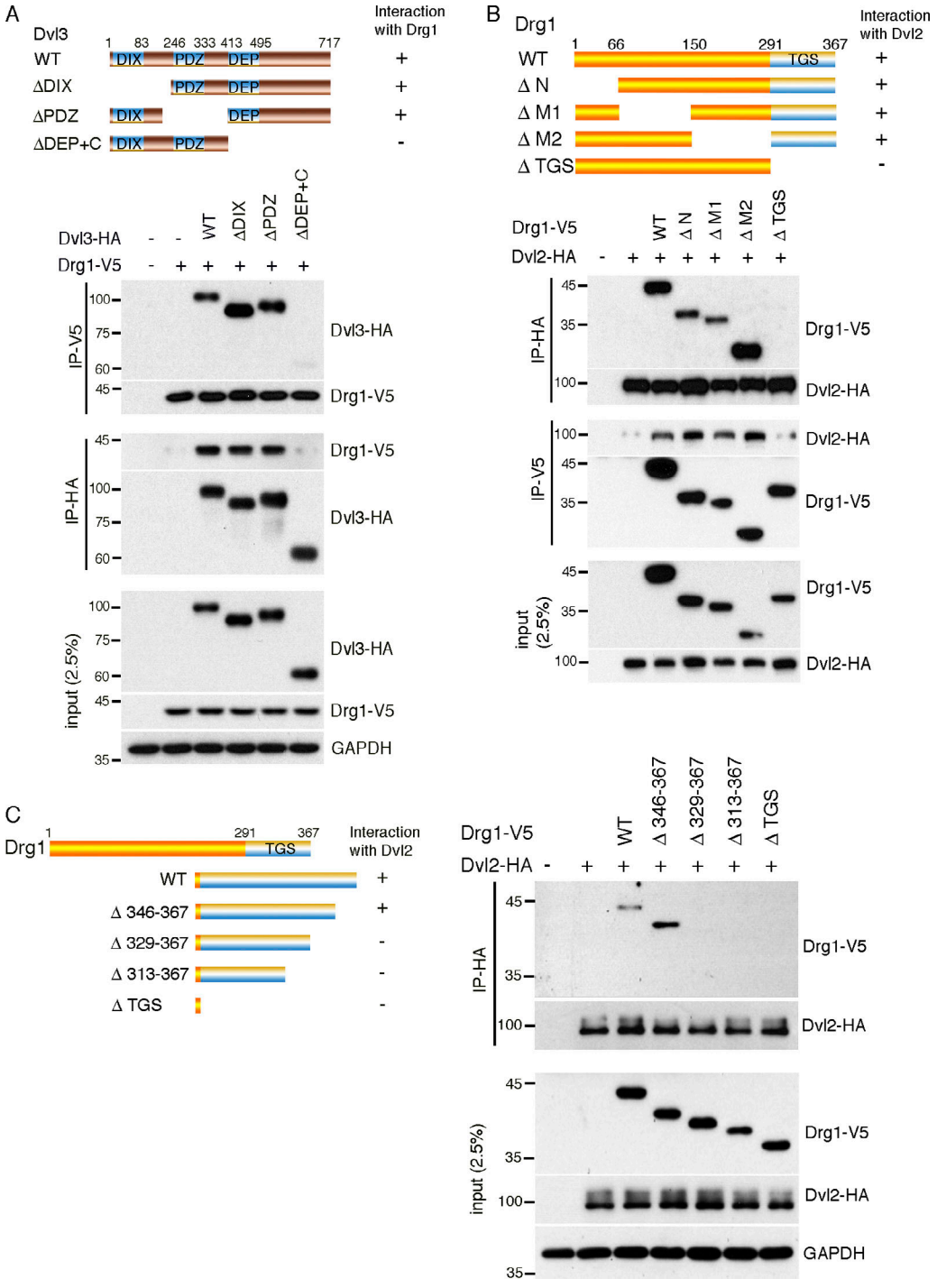

Figure S1. **Drg1–Dvl interaction domain mapping. (A)** Drg1 interaction domain mapping of Dvl3. The deletion mutants of Dvl3-HA and Drg1-V5 mRNAs were injected into embryos, and co-IP was performed. The Dvl3 DEP+C region is required for the Drg1 interaction. 2.5% of input was loaded. **(B)** Dvl2 interaction domain mapping of Drg1. mRNAs of Drg1 deletion mutants tagging V5 were coinjected with Dvl2-HA mRNAs. Dvl2-HA was precipitated by HA probe. The TGS domain is required for the Dvl2 interaction. 2.5% of input was loaded. ΔN, Δ1–65; ΔM1, Δ66–150; ΔM2, Δ151–290; ΔTGS, Δ291–367. **(C)** Amino acids 329–345 of Drg1 are necessary for Dvl2 binding. The indicated Drg1 deletion mutants tagged with V5 and Dvl2-HA mRNAs were used for co-IP experiments. Drg1 mutants harboring a deletion of amino acids 329–345 lost the interaction with Dvl2. 2.5% of input was loaded.

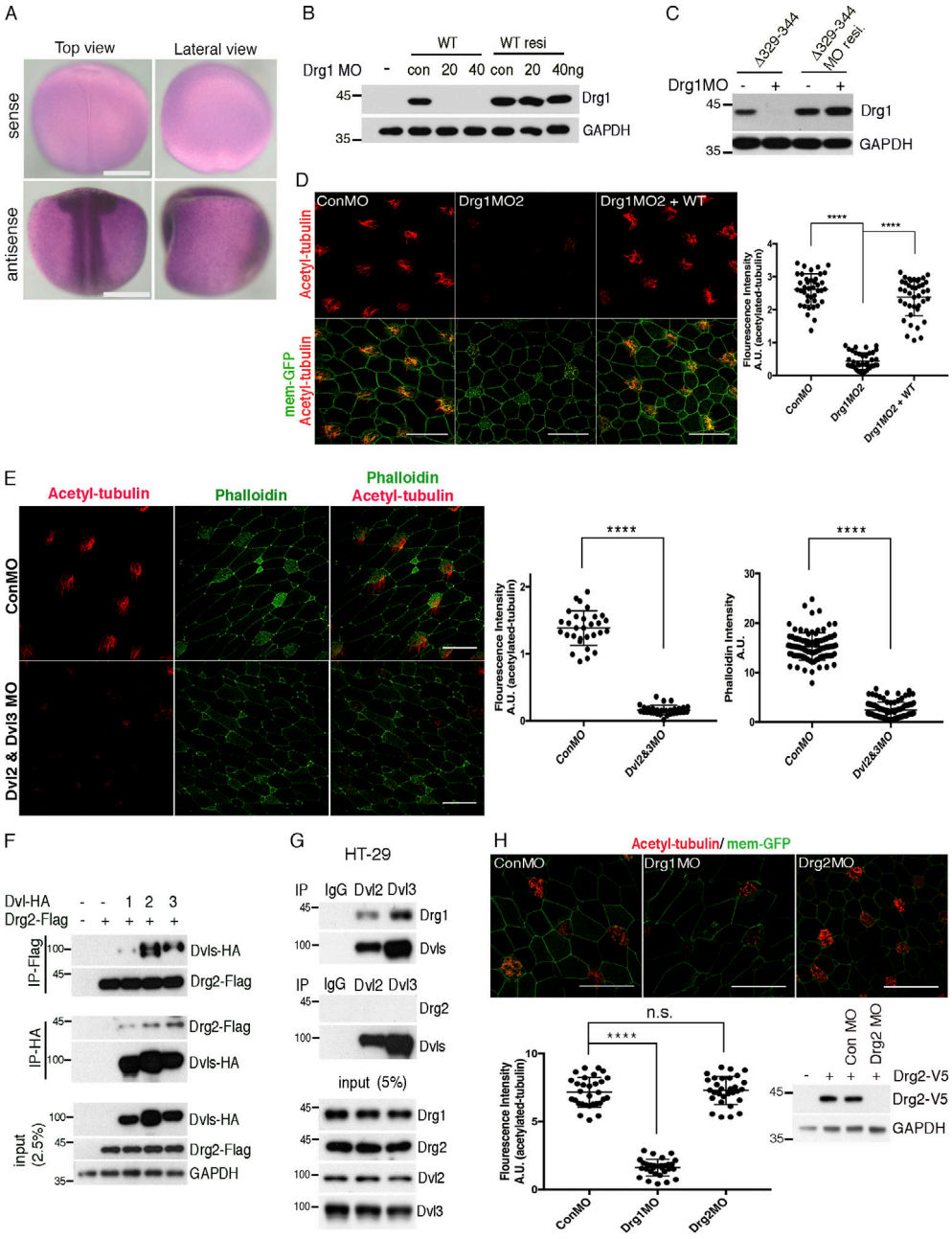

Figure S2. **Unlike Drg1 and Dvl, Drg2 is not required for multiciliation. (A)** Whole-mount in situ hybridization of Drg1. Embryos were fixed at stage 18. xDrg1 cDNA template from +1 to +1,104 was used to generate the sense and antisense RNA probes. Scale bars, 0.5 mm. **(B and C)** Verification of Drg1 MO and MO-resistant (MO resi) Drg1 mRNAs (WT and Δ329–344). To verify that the Drg1 MO prevents Drg1 translation, Drg1 MOs were coinjected with either WT Drg1 mRNA (sensitive to morpholino) or MO-resistant WT Drg1 mRNA (WT resi). For IB experiments, embryos were harvested at stage 12. **(D)** Decreased acetylated tubulin signal upon Drg1 knockdown with morpholino 2 (MO2). Embryos were injected with the indicated MOs and mRNA into both marginal ventral blastomeres at the four-cell stage. Embryos were fixed at stage 27, followed by immunostaining. Membrane-GFP (mem-GFP; green) was used as a tracer. Relative acetylated tubulin intensity is quantified (image n = 30 from 10 embryos for each condition). ****, $P < 0.0001$, one-way ANOVA. Scale bars, 50 µm. Error bars indicate ± SD. **(E)** Dvl2 and Dvl3 coknockdown results in decreased acetylated tubulin and apical actin (phalloidin) in MCCs. Either control MO or combined Dvl2 and Dvl3 MOs were injected into both ventral blastomeres in four-cell-stage embryos and harvested at stage 27 for immunostaining. Acetylated tubulin staining (red) represents multicilia, and phalloidin (green) indicates actin filaments. Relative acetylated tubulin and phalloidin intensities are quantified (image n = 30 from 10 embryos for acetylated tubulin, n = 98 for phalloidin in MCCs). ****, $P < 0.0001$, unpaired two-tailed t test. Scale bars, 50 µm. Error bars indicate ± SD. **(F)** Drg2 associates with overexpressed Dvl2 and Dvl3. The indicated mRNAs were injected, and embryos were harvested at stage 12 for co-IPs. 2.5% of input was loaded. **(G)** Reciprocal co-IPs of endogenous Drg2 and Dvl indicate that Drg2 does not associate with Dvl(s) in HT29 cells. 10% of input was loaded. **(H)** The indicated MOs were injected into both ventral blastomeres at the four-cell stage, and embryos were fixed at stage 27 for immunostaining. Unlike Drg1 knockdown, Drg2 knockdown does not affect acetylated tubulin staining in the MCCs. Relative acetylated tubulin intensity is quantified (image n = 30 from 10 embryos for each condition). ****, $P < 0.0001$, one-way ANOVA. Scale bars, 50 µm. Error bars indicate ± SD. To verify that the Drg2 MO prevents Drg2 translation, Drg2 MOs were coinjected with either WT Drg2 mRNA. For IB experiments, embryos were harvested at stage 12. a.u., arbitrary units; n.s., not significant.

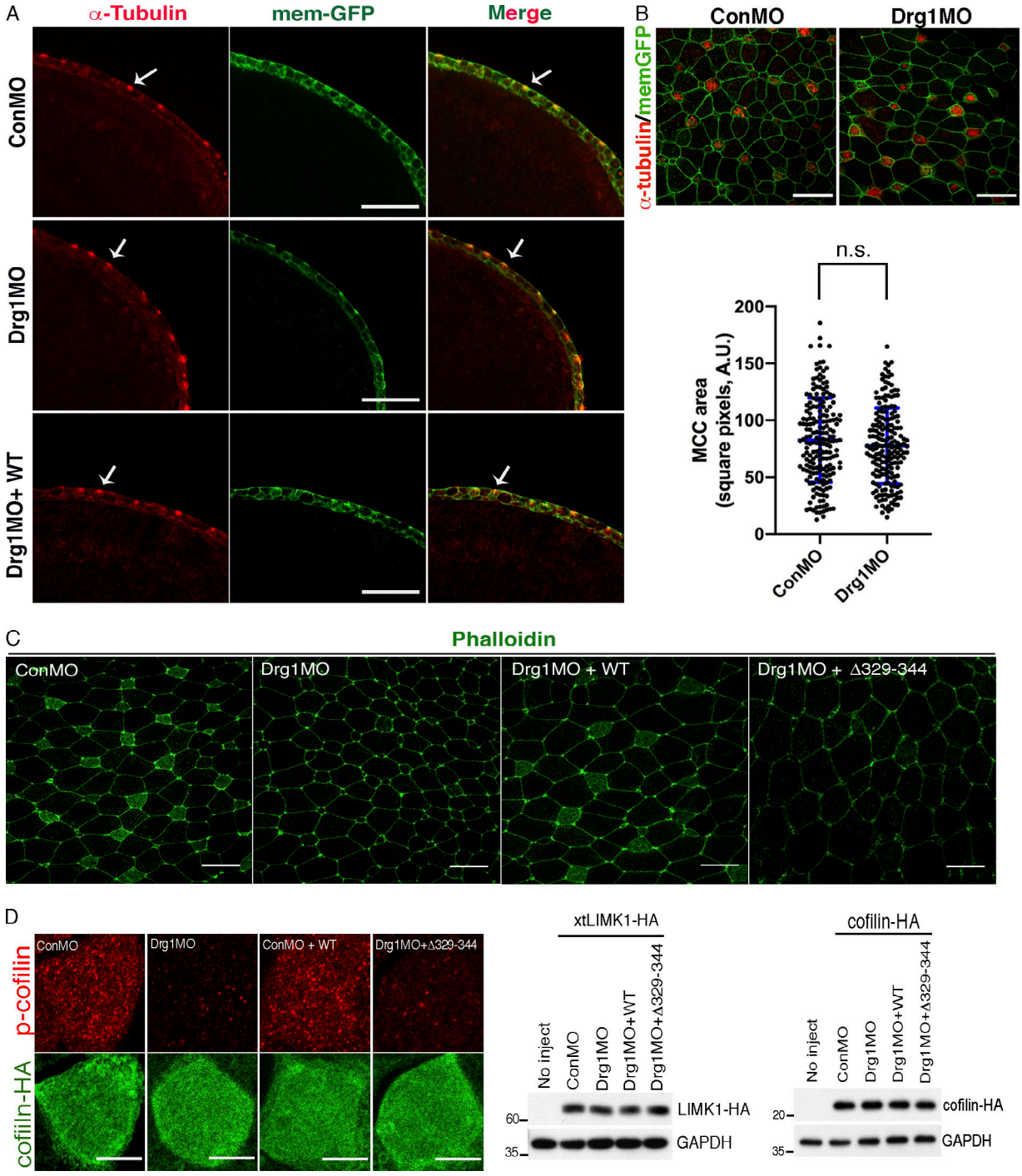

Figure S3. **Apical actin defects in Drg1 morphant MCCs is independent of MCC progenitor migration. (A)** Drg1 knockdown does not affect migration of MCC progenitors. At stage 25, epidermal ectoderm has MCCs that are distinguished by high intensity cell-interior α-tubulin IF (arrows point to one of these MCCs in each group). The MCCs migrated to the surface as shown in both the control morpholino-injected embryos and the Drg1 morphant and rescue group embryos. We observed <2% of MCCs that had not yet reached the surface ectoderm at this stage, regardless of Drg1 knockdown, in two independent experiments (control MO, 7 embryos, 2/105 IF-examined MCCs; MO, 8 embryos, 2/135 MCCs; rescue, 5 embryos 1/46 MCCs). Paraformaldehyde-fixed embryos were transverse sectioned and immunostained. Scale bar, 100 µm. **(B)** The indicated morpholinos and mem-GFP RNAs were injected to two ventral blastomeres of four-cell-stage embryos. α-tubulin IF was performed with stage 22 embryos, and the surface area of epidermal MCCs was measured. The number of measured MCCs, n = 190; embryos per group, n = 8; two-tailed unpaired t test. Error bars indicate ± SD. Scale bars, 50 µm. **(C)** Drg1 knockdown decreases apical actin staining in MCCs. The injected embryos fixed at stage 25 were used for phalloidin staining. Scale bars, 35 µm. **(D)** Drg1 knockdown does not affect total exogenous cofilin and LIMK1 proteins. mRNAs of cofilin-HA or LIMK1-HA were coinjected with the indicated mRNAs and MOs, and embryos were harvested at stage 12 for Western blot and at stage 25 for immunostaining. Scale bars, 5 µm. n.s., not significant.

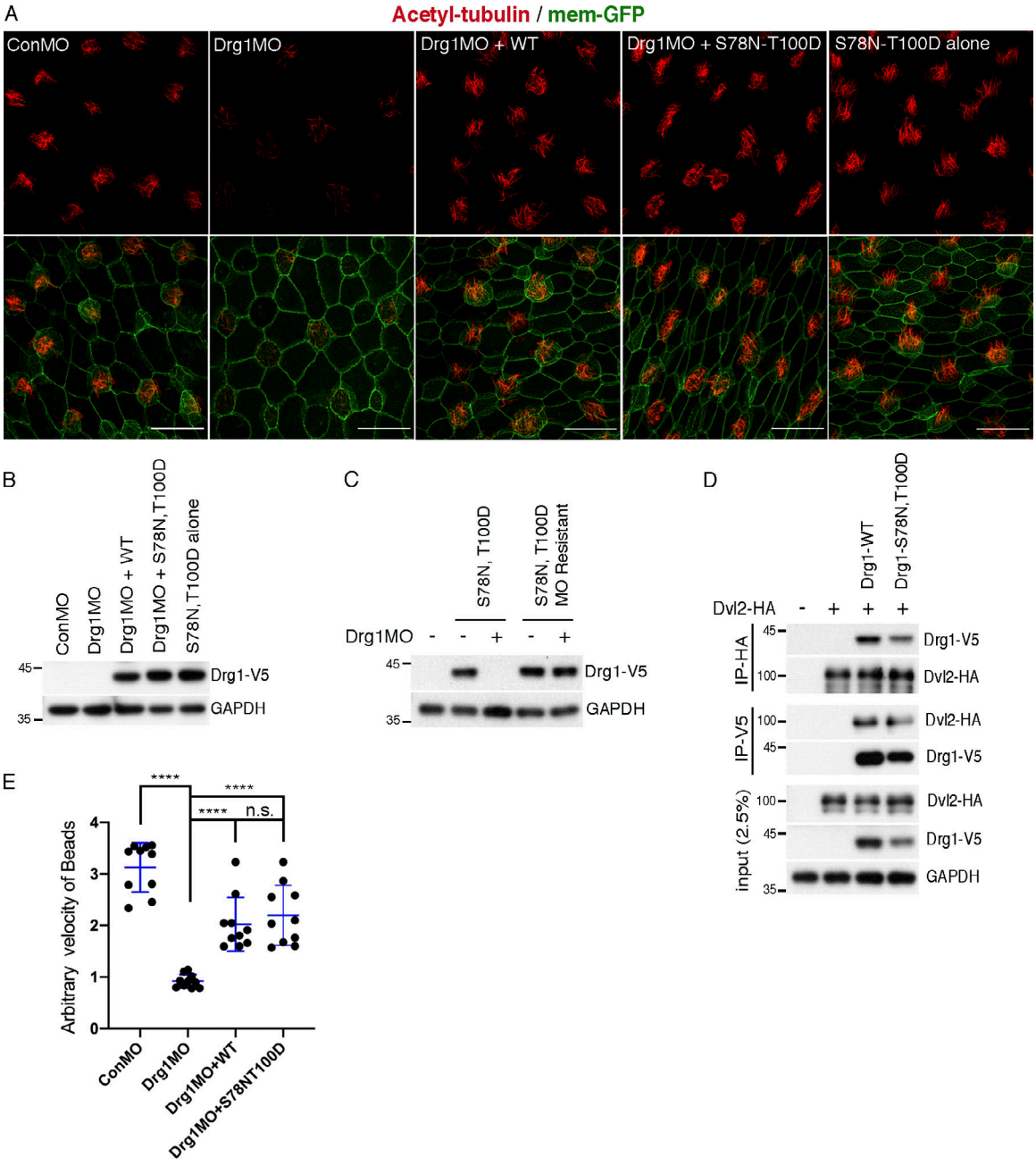

Figure S4. **Drg1 GTPase activity is not required for ciliation or cilia function in MCCs. (A)** Drg1 GTPase activity is dispensable for ciliogenesis in MCCs. The injected embryos with the indicated mRNAs and MOs were harvested at stage 27 and immunostaining was followed using anti-acetylated tubulin antibody and anti-GFP antibody. GFP is used as a tracer. Both Drg1 WT and the S78N-T100D mutant restores acetylated tubulin levels that were decreased upon Drg1 knockdown. Scale bars, 25 µm. **(B)** Immunoblots show similar protein expression levels between Drg1 WT and S78N-T100D. **(C)** Test of the MO-resistant S78N-T100 mutant. **(D)** Drg1 GTPase activity is not responsible for Drg1's interaction with Dvl2. The mRNAs of Drg1 WT and the double point mutant (S78N-T100D) were coinjected into embryos with Dvl2-HA mRNA, and co-IPs were conducted. **(E)** Quantification of the fluid flow with green fluorescent beads in Videos 4, 5, 6, and 7. Velocity of five beads along the body axis was manually measured. Measured bead velocity per embryo, *n* = 5; embryos (stage 27–28) per group, *n* = 10; stage 27 embryos; ****, P < 0.0001, one-way ANOVA. Error bars indicate ± SD. n.s., not significant.

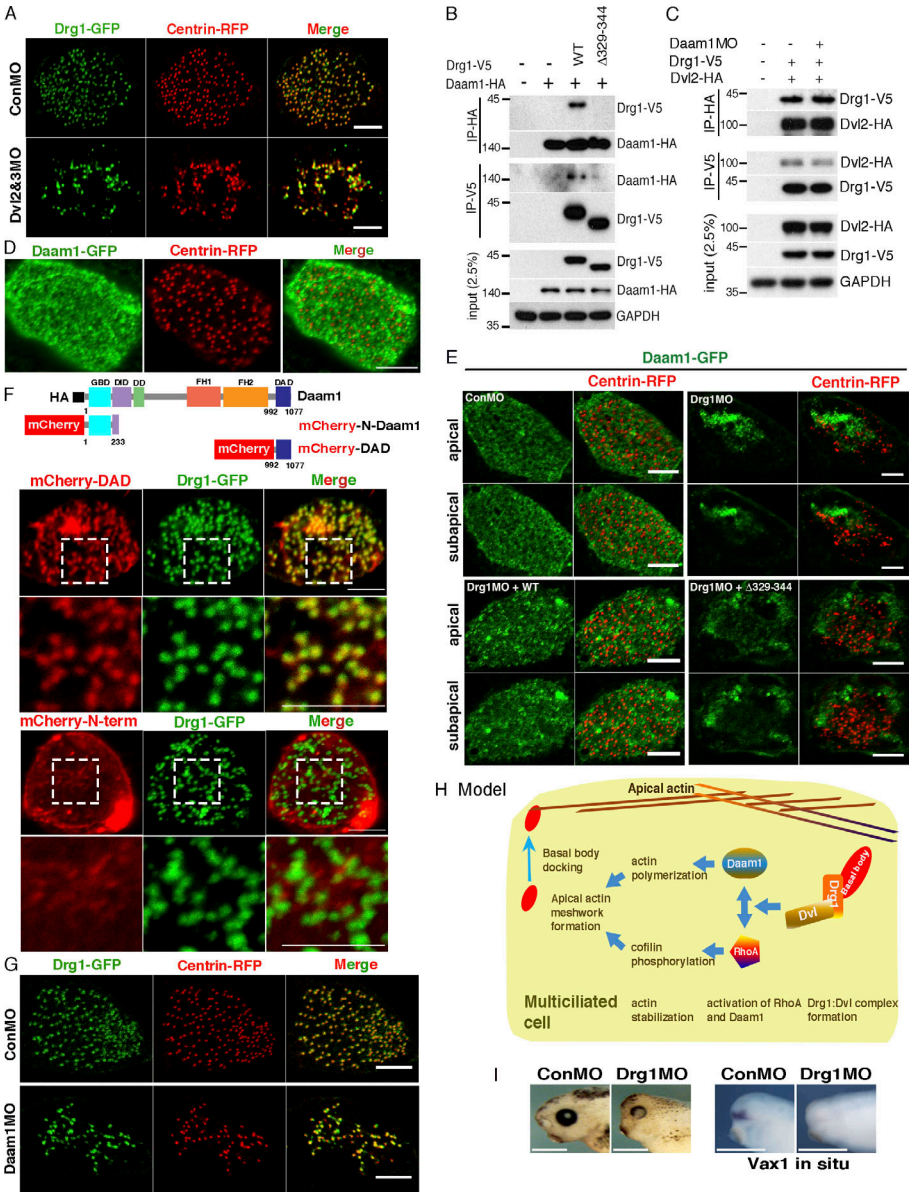

Figure S5. **Drg1–Dvl modulates multiciliation in cooperation with Daam1. (A)** Knockdown of both Dvl2 and Dvl3 did not affect Drg1 localization to the basal body area. The indicated MOs and mRNA cocktails were injected into both marginal ventral blastomeres of four-cell-stage embryos and fixed at stage 25. Images were generated by maximum intensity projection of serial z-stack confocal images. Scale bar, 5 µm. **(B)** Daam1 binds to Drg1 WT, but not Δ329–344. The mRNAs of Drg1-V5 (WT or Δ329–344) and Daam1-HA were coinjected into embryos and Co-IPs were performed. **(C)** Daam1 knockdown does not affect Drg1:Dvl2 association. Embryos injected with the indicated mRNAs and morpholinos were collected at stage 18 for co-IP experiments. **(D)** Daam1-GFP and centrin-RFP mRNAs were co injected and embryos were fixed at stage 25. Daam1-GFP heterogeneously localizes near and close to centrin-RFP in MCCs. Images are generated by maximum intensity projection of serial z-stack confocal images from surface (0 µm) to subapical (-1 µm) regions. Scale bars, 5 µm. **(E)** Drg1 knockdown causes irregular distribution of Daam1 in MCCs. Daam1-GFP and centrin-RFP mRNAs were coinjected with the indicated MOs and mRNAs into two ventral blastomeres of four cell stage embryos. Serial confocal images for MCCs were taken of embryos at stage 25. Apical and subapical indicate 0.5 µm and 1.0 µm from apical membrane, respectively. Images are representative of three independent experiments. Scale bars, 5 µm. **(F)** Drg1-GFP mRNAs were coinjected with the mRNAs encoding mCherry-DAD or mCherry-N-term into both ventral blastomeres of four cell stage embryos. mCherry-DAD, but not mCherry-N-term, localizes to Drg1-GFP in MCCs. The MCC images were taken from the epidermis of embryos at stage 25. Images are generated by maximum intensity projection of serial z-stack confocal images from surface to subapical regions. DD, dimerization domain; DID, diaphanous inhibitory domain; FH1, formin homology 1; FH2, formin homology 2; GBD, GTPase-binding domain. Scale bars, 5 µm. **(G)** The indicated MOs and mRNA cocktails were injected into both marginal ventral blastomeres of four-cell-stage embryos and fixed at stage 25. Knockdown of Daam1 did not affect Drg1 localization to the basal body area. Images are generated by maximum intensity projection of serial z-stack confocal images. Scale bars, 5 µm. **(H)** Model illustrating the roles of the Drg1 and Dvl interaction during ciliogenesis in MCCs. The Drg1–Dvl interaction drives Daam1 and RhoA activation. Then, active Daam1 stimulates actin polymerization and active RhoA leads to actin stabilization by cofilin phosphorylation downstream. The activation of RhoA affects Daam1 activation and vice versa. The resultant actin meshwork formation at MCCs contributes to basal body docking and subsequent ciliogenesis. **(I)** Drg1 knockdown causes phenotypes consistent with ciliary defects. The indicated morpholinos were injected into both dorsal blastomeres of four-cell-stage embryos. Images in the left two panels were taken at stage 42. For vax-1 (a sonic hedgehog downstream target), whole-mount in situ hybridization was performed on stage 35 embryos (right two panels). Scale bars, 0.5 mm.

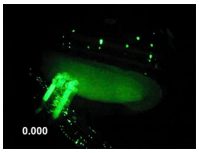

Video 1. **Ciliary fluid flow is not affected in control morphant embryos (see Fig. 2 F).** Ciliary fluid flow assay. Control morpholino–injected stage 27–28 embryos cultured in MBS. Fluorescent beads are dropped over the surface of the embryonic body in a glycerol solution, and normal flow from head to tail is observed due to ciliary movement. This video is presented in real time (30 frames per second [fps] on second clock display). Scale bar, 2 mm.

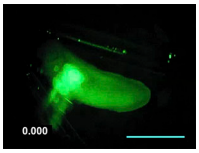

Video 2. **Ciliary fluid flow is markedly reduced in the absence of Drg1 (see Fig. 2 F).** Stage 27–28 embryos injected with Drg1 MO show little fluid flow in any direction when dropped upon the embryo surface. Arrowheads indicate some beads that just rest upon the embryo surface. This video is presented in real time (30 fps on second clock display). Scale bar, 2 mm.

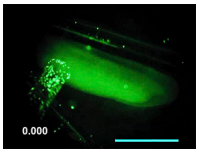

Video 3. **Rescue of ciliary function by re-expression of Drg1 in Drg1 morphant embryos (see Fig. 2 F).** Drg1 morpholino was injected along with MO-resistant Drg1RNA into embryos, and ciliary fluid flow was assessed at stage 27–28. The head-to-tail movement of beads along the body axis is restored by expression of Drg1 in the Drg1 morphant embryos. This video is presented in real time (30 fps on second clock display). Scale bar, 2 mm.

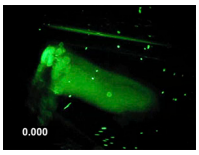

Video 4. **Ciliary fluid flow is not affected in control morphant embryos (see Fig. S4 E).** Control morpholino–injected stage 27–28 embryos were cultured in MBS. Fluorescent beads are dropped over the surface of the embryonic body in a glycerol solution, and normal flow from head to tail is observed due to ciliary movement. Movie is presented in real time (30 fps on second clock display). Scale bar, 2 mm. Videos 4, 5, and 6 are repeats of previous experimental groups (Videos 1, 2, and 3) but in a different experimental context that tests the effect of loss of Drg1 GTPase activity on ciliary function.

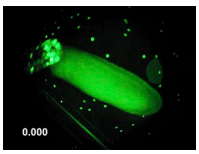

Video 5. **Ciliary fluid flow is markedly reduced in the absence of Drg1 (see Fig. S4 E).** Stage 27–28 embryos injected with Drg1 MO exhibited slower bead flow in any direction when dropped upon the embryo surface. This video is presented in real time (30 fps on second clock display). Scale bar, 2 mm.

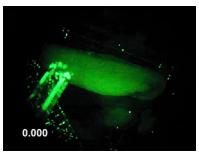

Video 6. **Rescue of ciliary function by re-expression of Drg1 in Drg1 morphant embryos (see Fig. S4 E).** Drg1 morpholino was injected along with MO-resistant Drg1RNA into embryos and ciliary fluid flow was assessed at stage 27–28. The head-to-tail movement of beads along the body axis is restored by expression of Drg1 in the Drg1 morphant embryos. This video is presented in real time (30 fps on second clock display). Scale bar, 2 mm.

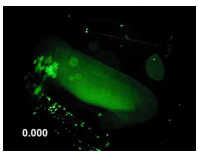

Video 7. **Rescue of ciliary function in Drg1 morphant embryos by expression of a GTPase mutant Drg1 harboring two mutations (S78N-T100D; see Fig. S4 E).** Drg1 morpholino was injected along with MO-resistant mutant Drg1RNA (S78N-T100D) into embryos, and ciliary fluid flow was assessed at stage 27–28. The head-to-tail movement of beads along the body axis is restored by expression of mutant Drg1 (S78N-T100D) in the Drg1 morphant embryos, similar to that of WT Drg1. This video is presented in real time (30 fps on second clock display). Scale bar, 2 mm.

Provided online is one supplemental table in Excel. Table S1 shows a list of proteins detected in the mass spectrometric analysis of Dvl2 IPs from Xenopus embryos expressing Dvl2.